Permeability of Filter Cakes of Palm Oil in Relation to Mechanical Expression

G. F. Kamst, O. S. L. Bruinsma, and J. de Graauw
Laboratory for Process Equipment, Delft University of Technology, 2628 CA Delft, The Netherlands

Permeability and compressibility data are required for an adequate process model for compressible-cake filtration and mechanical expression. Experimental and modeling results of the permeability of palm-oil filter cakes (a highly compressible viscoelastic material) are combined with compressibility data, leading to a model for the expression step. Permeability measurements show that permeability depends strongly on the quantity of fine particles in the cake. Removal of fine particles from the slurry before expression significantly increases the solid-phase content during expression due to higher permeability. Modeling results of the expression step show that for palm-oil filter cakes there is a pressure above which the attainable mass fraction of solids becomes independent of pressure. Decrease in specific cake resistance has two effects: a higher mass fraction of solids at the same pressure and a higher pressure at which the mass fraction of solids is not affected further.

Introduction

Cake filtration and expression are widely applied in the field of chemical technology. For the optimization of the filtrate flow or the solid-phase content, a predictive model is often needed. Compressible-cake filtration and expression are usually modeled with theories based on mass and momentum balances. A general approach for the modeling of compressible-cake filtration and expression was given by Tiller and Yeh (1987) and Stamatakis and Tien (1991). This approach leads to an equation with a material-independent part, which is based on mass and momentum balances of the liquid and solid phase, and with a material-dependent part, which is based on the permeability and the compressibility of the bulk material. For the modeling of compressible-cake filtration and expression, information about the bulk permeability and compressibility must therefore be available.

A method that is often applied for the measurement of the compressibility and permeability is based on the compression–permeability cell. The compression–permeability cell is an apparatus in which a solid/liquid mixture can be subjected to an externally applied pressure while liquid is pressed through the cake at a constant pressure. For materials that do not show viscoelastic behavior, the liquid flow will decrease in time until it becomes constant. If the liquid pressure drop is low compared to the externally applied pressure, the local liquid pressure gradient, superficial liquid velocity, and porosity are equal to the global values and, therefore, the permeability can be determined. In the case of viscoelastic materials the liquid flow may not reach an equilibrium value. However, a liquid velocity that is constant as a function of time is not an essential condition for determining the permeability. If the liquid velocity due to consolidation of the cake is low compared to the inlet velocity, then the liquid velocity is practically not a function of the position in the cake, and there are no gradients of the solid compressive pressure and porosity. From this it follows that the permeability of cakes of viscoelastic materials can also be measured.

In a recent article (Kamst et al., 1996) results of the measurement of creep curves of palm-oil filter cakes were described. In this article, we present experimental and modeling results of the permeability of palm-oil filter cakes. The permeability of a filter cake can be strongly dependent on the particle-size distribution, especially on the content of small particles or *fines* (Tien, 1991). A small change in the fines content may therefore lead to a significant change of the solid-phase content after expression. In this article, we also study these effects. These results are combined with previously obtained compressibility measurements and a theory based on mass and momentum balances, leading to a model for the expression step.

Correspondence concerning this article should be addressed to J. de Graauw.

Theory of Consolidation

Mass balance

For the flow of liquid through a compressible porous medium the following mass balance can be derived (Shirato et al., 1986; Smiles and Kirby, 1987):

$$\frac{\partial e}{\partial t} = -\frac{\partial q}{\partial \omega}, \tag{1}$$

with
e = void ratio
t = time (s)
q = superficial liquid velocity relative to the solid velocity (m/s)
ω = volume of solid phase between the position in the cake x and the filter, divided by the filter area (m)

The relation between the moving spatial coordinate ω and the fixed coordinate x is as follows:

$$d\omega = (1-\phi)\,dx, \tag{2}$$

where ϕ is the porosity. Because the volume of the solid phase in a slice, $d\omega$, is constant, the use of the coordinate ω instead of x will lead to time-independent boundaries during simulation. The void ratio e is related to the porosity by the following equation:

$$e = \frac{\phi}{1-\phi}. \tag{3}$$

The relative superficial liquid velocity q is defined as

$$q = \phi(w - v_s) \tag{4}$$

where w and v_s are the absolute liquid- and solid-phase velocities, defined as positive in the direction of the spatial coordinate x.

Momentum balance

If the inertial terms and the fluid-phase viscous term can be neglected, the momentum balance for the liquid and the solid phases is as follows (Chase and Willis, 1992; Willis et al., 1983):

$$\frac{\partial p_l}{\partial x} + \frac{\partial p_s}{\partial x} - \rho_l g - (1-\phi)(\rho_s - \rho_l)g = 0, \tag{5}$$

with
p_l = liquid pressure (Pa)
p_s = solid compressive pressure (Pa)
ρ_l = liquid-phase density (kg/m^3)
ρ_s = (intrinsic) solid phase density (kg/m^3)
g = gravitation acceleration, defined as negative in the positive x-direction (m/s^2)

If the pressure gradient due to gravitation can be neglected compared to the liquid and solid pressure gradients, the momentum balance becomes

$$\frac{\partial p_l}{\partial x} + \frac{\partial p_s}{\partial x} = 0. \tag{6}$$

Equations defining compressibility and permeability

Besides mass and momentum balances, equations for the compressibility and permeability of the cake are necessary. Both are dependent on the characteristics of the expressed material. In the case of laminar flow, the relation between liquid velocity and liquid pressure drop can be described by Ruth's modification of Darcy's law:

$$q = -\frac{1}{\mu\alpha\rho_s}\frac{\partial p_l}{\partial \omega}, \tag{7}$$

where α is the specific cake resistance (m/kg) and μ is the dynamic liquid viscosity (Pa·s). The specific cake resistance is dependent on the size and shape of the particles and the cake porosity.

The compressibility can be defined by the following equation (Moore, 1972):

$$\beta = -\frac{1}{V}\left(\frac{\partial V}{\partial p_s}\right)_T = -\frac{1}{1+e}\frac{\partial e}{\partial p_s}, \tag{8}$$

with
β = compressibility (Pa^{-1})
T = temperature (K)
V = cake volume (m^3)

The compressibility β is usually dependent on the void ratio.

Consolidation equation

The combination of Eqs. 1, 2, 6, 7 and 8 results in the following equation:

$$\frac{\partial e}{\partial t} = \frac{\partial}{\partial \omega}\left(C_e\frac{\partial e}{\partial \omega}\right), \tag{9}$$

where C_e is defined as

$$C_e = \frac{1}{\mu\alpha\rho_s(-\partial e/\partial p_s)}. \tag{10}$$

Mathematically, this equation resembles a nonstationary diffusion equation. It is a second-order partial differential equation, and therefore requires that one initial condition and two boundary conditions be defined. From experiments (Kamst et al., 1995) it appeared that the filter cake was homogeneous before expression. This result was used as an initial condition for the simulations. The boundary conditions for expression with a single drainage surface are given in Table 1, where ω_0 denotes the total solids volume divided by the filtration area and p is the external load.

Table 1. Boundary Conditions for an Expression Process with One Drainage Surface

Position	Solid Compressive Pressure p_s	Void Ratio e
Filter ($\omega = 0$)	$p_s = p$	$e = f(p,t)$
Piston ($\omega = \omega_0$)	$\partial p_s/\partial\omega = 0$	$\partial e/\partial\omega = 0$

Experimental Procedure

Permeability measurements have been carried out with both air and liquid. Refined palm-oil was used for the experiments. The oil was crystallized by batch in a 4-L stirred vessel. The end temperature of the crystallization step was 28°C, leading to a mass fraction of solids of 10–11%. The crystallization conditions were kept identical for every experiment.

Measuring the cake permeability with air instead of liquid has the advantage that the air flow is much higher than the liquid flow at the same pressure drop. This is based on the much lower viscosity of air compared to liquid palm oil. If the flow remains laminar, Darcy's law can be applied. For the air permeability measurements, the liquid content of the cake must be as low as possible, because the presence of liquid leads to an increase in the flow resistance. Detergent-washed particles were used for the measurements; these particles were also used for the measurement of creep curves (Kamst et al., 1996).

During the air permeability measurements, the air pressure and flow were measured with an electronic pressure sensor and a mass-flow sensor/controller. The effect of the washing procedure on the particle-size distribution was studied with a Malvern particle-size analyzer.

For the permeability measurements with liquid, filtrate obtained from palm-oil slurry (palm olein) was used. The equipment for these experiments is shown in Figure 1. The diameter of the perspex column was 60 mm. The inlet flow and the cake thickness were measured with a mass flowmeter and a displacement meter, respectively. The mass of filtrate was recorded with a balance. Different volume fractions of solids, and therefore different specific cake resistances, were obtained by varying the externally applied pressure and the liquid pressure.

To verify the model for the expression step, expression experiments have been carried out with the equipment shown in Figure 1. The filtration of the slurry was carried out at a constant pressure drop of 1 bar, using a 15-μm cloth, which was also used for the expression step. The expression experiments were carried out at various expression times, solids loads, and externally applied pressures. After expression, the mass fraction of solids was measured with a Bruker minispec low-resolution pulse nuclear magnetic resonance (NMR) apparatus (type pc120), which is a common apparatus for determining the mass fraction of solids of edible fats. In a number of experiments, the mass fraction of solids was measured as a function of the axial position, by cutting the cake into slices. The minimum slice thickness that could be obtained was about 0.4 mm. The slice thickness was calculated from the mass and mass fraction of solids of the slice.

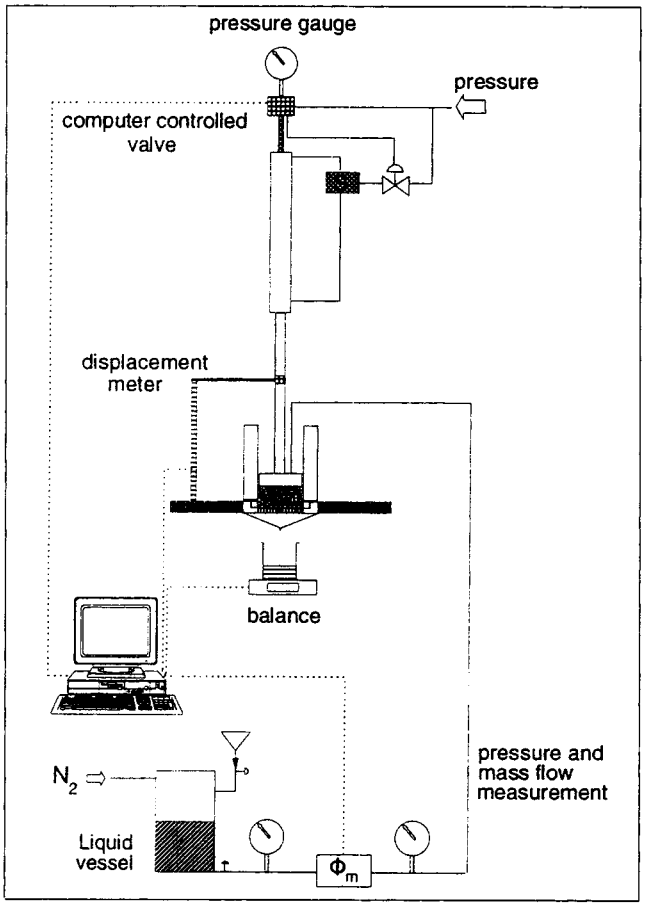

Figure 1. Equipment for the permeability measurements with liquid.

Experimental Results

Permeability measurements

Figure 2 shows the results of a permeability measurement with air. Although not all of the liquid in the cake can be removed during detergent washing, no liquid was expressed during the permeability measurement. From Figure 2 it appears that the specific cake resistance is very strongly dependent on the volume fraction of solids; an 18% increase in the volume fraction of solids leads to a factor of 10^4 increase in the specific cake resistance.

Figure 3 shows the difference between the inlet and outlet flows as a function of time during a permeability experiment with liquid. It appears that after a certain period of time (5 hours by average, depending on the externally applied pressure) the inlet and the outlet flows become equal. From this it follows that the flow due to consolidation of the cake becomes negligible with respect to the inlet flow, which is a requirement to obtain reliable specific cake-resistance values.

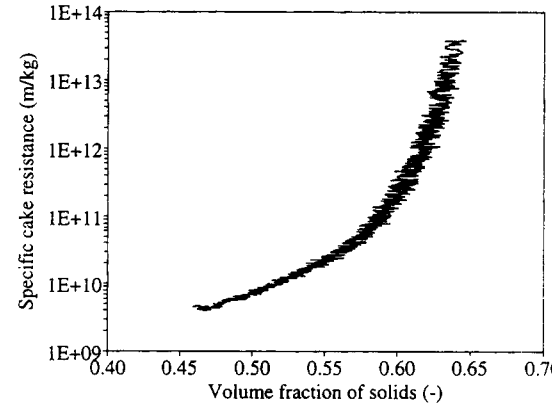

Figure 2. Example of a permeability measurement with air.

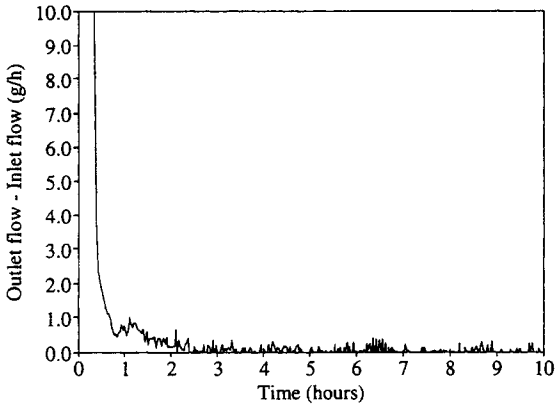

Figure 3. Difference between inlet and outlet flows for a permeability measurement with liquid.

$p_l = 0.13$ bar, $p = 0.89$ bar.

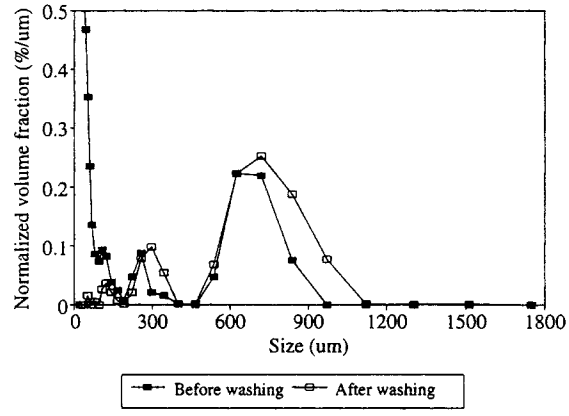

Figure 5. Particle size distributions before and after detergent washing.

However, the flow does not become constant, due to continuing creep of the solid phase (Kamst et al., 1996). Figure 4 contains the results of various liquid permeability measurements. The specific cake-resistance values were calculated from the flow as a function of time and the liquid pressure drop. The figure shows the specific cake-resistance values for volume fractions of solids from the time when the entrance and outlet flows become equal until the end of the experiment (22 to 24 hours). It appears that the specific cake resistance is not a function of the porosity only. The specific cake resistance increases faster during one experiment than would be expected from the results of different experiments. The strongly increasing specific cake resistance during one experiment follows from the decreasing flow at a barely increasing volume fraction of solids. During the experiments the specific cake resistance increases with a factor of 2.5 by average. The duration of a permeability measurement (22 to 24 hours) is much longer than the duration of a normal expression experiment (1 hour), and the flow through the cake is much higher. Therefore, the increasing resistance is probably caused by migration of the fines toward the filter or the blocking of the filter cloth by fines.

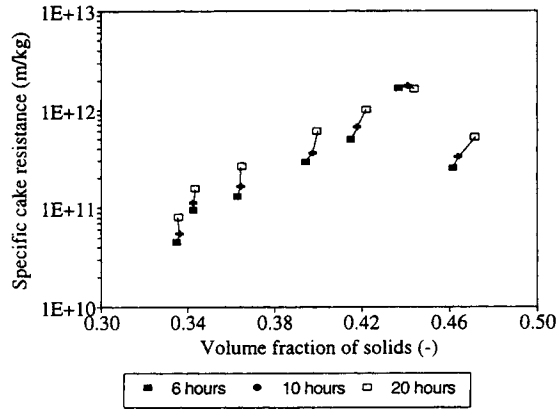

Figure 4. Specific cake resistance as a function of the volume fraction of solids, measured with liquid.

The separate curves originate from different experiments.

If the results of Figure 4 are compared with Figure 2, it appears that the specific cake resistance measured with liquid is about a factor of 200 higher than the specific cake resistance measured with air. In Figure 5 representative particle-size distributions are shown before and after detergent washing of the cake. It appears that after washing the sample contains hardly any particles with sizes smaller than 150 μm, which is not the case for the sample before washing. These particles probably disappear by agglomeration or by passing through the filter during the washing procedure. It is well known that the fines content can significantly influence the filtration rate. The decrease in the specific cake resistance due to washing is most likely caused by removal of the fine particles.

Classification experiments

From the results mentioned in the previous paragraph it follows that the permeability of the unwashed cake can be increased by removing the fines, which can lead to a higher solid-phase content during expression. To verify this hypothesis, experiments were carried out to classify the slurry before filtration and expression. Two methods of classification were used:

- After slurry sedimentation, several layers of solids can be distinguished. The upper layers, containing the fine particles, were drawn off by suction. This fraction was filtered across a cloth with small pores (15 μm). The clear palm olein obtained was added to the slurry from which the fines were removed.
- The slurry was filtered across a filter cloth with wide pores (600 μm). The fine particles passed through the filter. The palm olein with the fines was filtered across a filter cloth with small pores. The filtered clear olein was added to the slurry from which the fines were removed.

After classification, the slurry was filtered and expressed at various pressures for 1 hour. Besides experiments where fines were removed from the slurry, expression experiments with unclassified slurry were also carried out. These reference experiments were carried out with an equal mass of solid phase, to eliminate the effect of the solids mass on the solid-phase content. Also, we studied the effect of classifying the slurry on particle-size distribution.

Table 2. Conditions of the Classification Experiments and Expression Results

Exp. No.	Classification Method	p bar	$x_{s,c}$	$x_{s,\mathrm{ref}}$	Δx_s
1	Drawing off by suction	7.1	0.538	0.523	0.015
2	Drawing off by suction	7.1	0.555	0.530	0.025
3	Drawing off by suction	8.9	0.549	0.514	0.035
4	Drawing off by suction, followed by single filtration across cloth with wide pores	10.7	0.567	0.507	0.060
5	Drawing off by suction followed by 2 times filtration across cloth with wide pores	10.7	0.547	0.487	0.060
6	Drawing off by suction, followed by 3 times filtration across cloth with wide pores	10.7	0.568	0.492	0.076

The experimental conditions and the resulting mass fraction of solids after expression are shown, for both classification experiments and reference experiments, in Table 2. The symbols in the table have the following meaning:

$x_{s,c}$ = mass fraction of solids after classification and expression during 1 hour

$x_{s,\mathrm{ref}}$ = mass fraction of solids without classification, after expression during 1 hour

Δx_s = difference between the mass fractions of solids with and without classification before expression

It appeared from a mass balance that during classification about 25% of the pure solids mass is removed. In Figure 6 particle-size distributions before and after classification by suction (experiment 2) are shown. It appears that after suction, the slurry contains fewer particles smaller than 200 μm. Also a portion of the larger particles is removed, but since Figure 6 shows a (normalized) volume-based distribution, the number of these particles is relatively small.

From Table 2 it appears that classification before expression always leads to a mass fraction of solids that is higher than in the reference experiments, which were carried out with an equal mass of solid phase. From this it follows that the higher mass fraction of solids after expression is a consequence of fines removal. The influence of classification on the mass fraction of solids after expression increases significantly with the externally applied pressure. It also follows from Table 2 that the number of filtration stages across a filter with wide pores may not have a significant additional effect.

Modeling of the Permeability Results

There is no general theory for the permeability of particulate beds. Models with a theoretical basis are the Kozeny-Carman equation, the free-surface model of Happel (1958), and the equation derived by Rumer (De Wiest, 1969). None of these models could describe the experiments adequately. It was stated by Grace (1953) that the permeability of compressible cakes cannot generally be described by the Kozeny-Carman equation. Because there is no appropriate theoretical model that can describe the permeability of palm-oil filter cakes, an empirical model is used. Barends (1994) suggested the following equation:

$$K = K_0 \cdot \exp[d(\phi - \phi_0)], \tag{11}$$

with

K_0 = permeability at porosity ϕ_0 (m^2)

d = empirical parameter

This equation was modified as follows:

$$\alpha = \alpha_0 \cdot \exp[d(\phi_0 - \phi)], \tag{12}$$

where α_0 is the specific cake resistance at the initial porosity ϕ_0 (m/kg). Figure 7 shows the fit of this equation and the experimental data. The following values for α_0 and d were obtained:

$$\alpha_0 = (1.3 \pm 0.3) \times 10^9 \text{ m/kg}$$

$$d = 31 \pm 3$$

During the experiments the initial porosity (ϕ_0) appeared to be 0.8; this value was also used for the fit of Eq. 12. The value of d is high compared to the d value of soils (which ranges from 0 to 7) (Barends, 1994), from which it follows that the dependency of the specific cake resistance on the volume fraction of solids is extremely high.

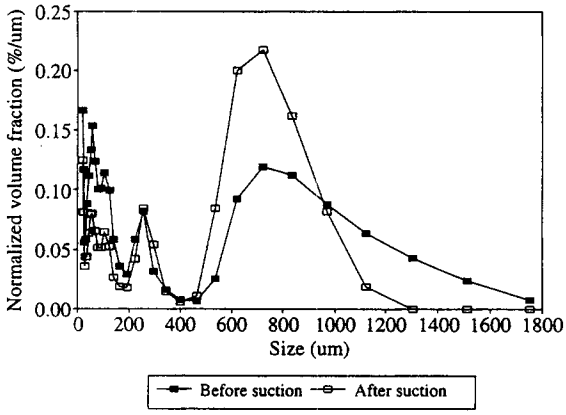

Figure 6. Particle size distributions before and after fines removal by suction, carried out after sedimentation of the slurry.

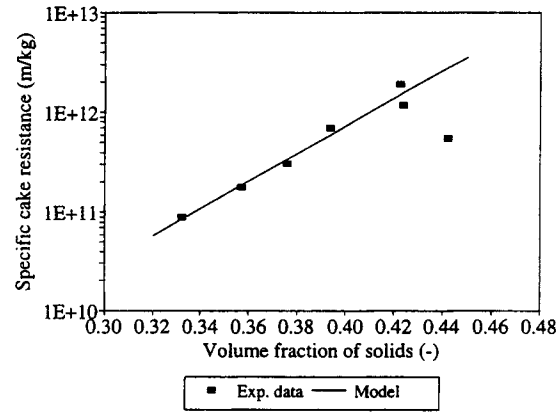

Figure 7. Liquid permeability data with the fit of Eq. 12.

$\alpha_0 = 1.3 \times 10^9$ m/kg and $d = 31.64$.

Modeling of the Expression Step

Basic equations

Besides the partial differential equation for consolidation (Eq. 9) and a relation between the specific cake resistance and the porosity (Eq. 12), information about the cake compressibility is also required. The following relation between the void ratio and the solid compressive pressure was used, which was obtained from creep measurements of palm-oil filter cakes (Kamst et al., 1996):

$$\ln\left(\frac{e}{e_0}\right) = a\left(\frac{p_s}{p_{s,\mathrm{ref}}}\right)^b\left(\frac{t}{t_{\mathrm{ref}}}\right)^c, \tag{13}$$

with

e_0 = void ratio at $t = 0$
$p_{s,\mathrm{ref}}$ = reference pressure (= 1 bar)
p_s = solid compressive pressure (bar)
t_{ref} = reference time (= 1 s)
a, b, c = empirical parameters

The empirical parameters were found to have the following values:

$$a = -0.489 \pm 0.014;$$
$$b = 0.563 \pm 0.0262;$$
$$c = (4.65 \pm 0.30) \times 10^{-2}.$$

The local void ratio is not only dependent on the actual pressure and time, but also on the pressure history. Since the solid compressive pressure at a fixed position in the cake is not constant during expression of a wet solid, it is necessary to have a model for the pressure history effect on the creep curve. The creep curves of palm-oil filter cakes at time-dependent pressures can be predicted from the creep curves at constant pressures by the strain-hardening model (Kamst et al., 1996):

$$\epsilon[p_s(t), t] = \sum_{i=1}^{N} [f(p_{s,i}, t_i - t_{i-1} + \tau_{i-1}) - f(p_{s,i}, \tau_{i-1})], \tag{14}$$

with

N = number of time intervals
$\epsilon[p_s(t), t]$ = natural strain at a time t and a time-dependent pressure
$f(p_s, t)$ = natural strain as a function of time at a constant pressure
τ_{i-1} = the time needed to obtain the present strain $[\epsilon(p_{s,i-1}, t_{i-1})]$ at the new pressure $(p_{s,i})$ (s)

In this equation t_0 and τ_0 are zero by definition. The natural strain is defined by the following equation (Barends, 1980):

$$d\epsilon = \frac{dV}{V} \Rightarrow \epsilon = \ln\left(\frac{V}{V_0}\right), \tag{15}$$

where V_0 is the cake volume at $t = 0$. Assuming that the intrinsic solid-phase density ρ_s is constant, the following relation can be derived using a mass balance of the solid phase and Eq. 3:

$$\epsilon = \ln\left(\frac{1+e}{1+e_0}\right). \tag{16}$$

The function $f(p_s, t)$ follows when Eqs. 13 and 16 are combined.

Solution procedure

The strain-hardening model (Eq. 14) predicts the strain at a time t_i from the pressure at a time t_i and the strain at a time t_{i-1}. To calculate the strain at the time t_i, the pressure at t_i must be known. The strain-hardening model cannot be used if the pressure must be calculated from the strain value, because τ_{i-1} is a function of the unknown pressure $p_{s,i}$, resulting in an equation with two unknowns. Therefore, Eq. 9 cannot be solved with e as the dependent variable, and must be written as a function of p_s.

If the solid phase shows creep, the void ratio is an explicit function of time and solid compressive pressure:

$$e = e[p_s(t, \omega), t]. \tag{17}$$

The solid compressive pressure is a function of time and position, and the void ratio is therefore also an implicit function of the position in the cake. The derivatives of Eq. 17 with respect to time and position are (Bronwell, 1953)

$$\left(\frac{\partial e}{\partial t}\right)_\omega = \left(\frac{\partial e}{\partial p_s}\right)_t \left(\frac{\partial p_s}{\partial t}\right)_\omega + \left(\frac{\partial e}{\partial t}\right)_{p_s} \tag{18}$$

$$\left(\frac{\partial e}{\partial \omega}\right)_t = \left(\frac{\partial e}{\partial p_s}\right)_t \left(\frac{\partial p_s}{\partial \omega}\right)_t. \tag{19}$$

Because the mass balance (Eq. 1) is derived for constant ω, the partial derivative $\partial e/\partial t$ in Eq. 9 is equal to $(\partial e/\partial t)_\omega$. Rewriting Eq. 18 in terms of $(\partial p_s/\partial t)_\omega$, followed by combining it with Eqs. 9, 10, and 19, leads to:

$$\left(\frac{\partial p_s}{\partial t}\right)_\omega = \frac{\dfrac{\partial}{\partial \omega}\left[-\dfrac{1}{\mu\alpha\rho_s}\cdot\left(\dfrac{\partial p_s}{\partial \omega}\right)_t\right]}{\left(\dfrac{\partial e}{\partial p_s}\right)_t} - \frac{\left(\dfrac{\partial e}{\partial t}\right)_{p_s}}{\left(\dfrac{\partial e}{\partial p_s}\right)_t}. \tag{20}$$

The righthand side of this equation consists of a diffusive term and a source term, respectively. If the material does not show creep, the source term will be zero. The values of $(\partial e/\partial t)_{p_s}$ and $(\partial e/\partial p_s)_t$ can be obtained by differentiation of Eq. 13. Equation 20 was solved numerically with the finite difference method, using an explicit difference scheme, leading to the solid compressive pressure distribution in the cake. The porosity distribution was obtained by combining the p_s-distribution with Eqs. 13, 14, and 16.

Modeling results

A simulation of the expression step is shown in Figure 8, with the fit values obtained from the data shown in Figure 7. It appears that for these values of α_0 and d the simulated

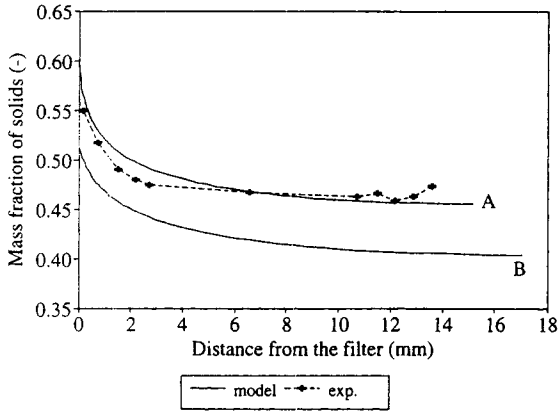

Figure 8. Influence of parameter α_0 on the fit of Eq. 12.

α_0 values (m/kg): A: 0.35×10^9, B: 1.31×10^9 (original value); $d = 31.64$; expression time = 3,600 s; solids load = 7.07×10^{-3} $m^3_{solids}/m^2_{filter}$; pressure = 10.7 bar.

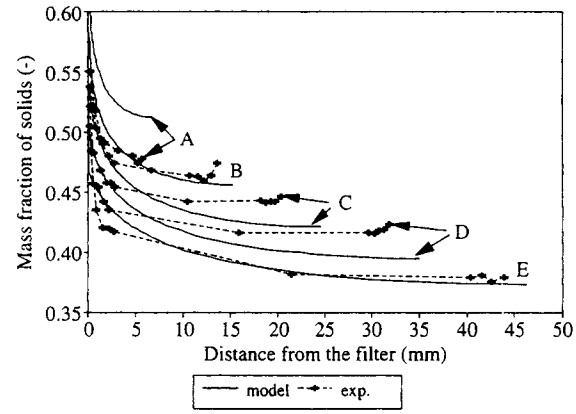

Figure 10. Simulations using Eq. 12 with $\alpha_0 = 0.35\times10^9$ m/kg vs. experiments as a function of the solids load ω_0 (in $m^3_{solids}/m^2_{filter}$).

A: $\omega_0 = 3.5\times10^{-3}$; B: $\omega_0 = 7\times10^{-3}$; C: $\omega_0 = 10.5\times10^{-3}$; D: $\omega_0 = 14\times10^{-3}$; E: $\omega_0 = 17.5\times10^{-3}$. Expression time = 3,600 s; pressure = 10.7 bar.

mass fraction of solids is too low compared to the experiment. From Figure 4 it appeared that the specific cake resistance increases faster during an experiment than would be expected from the results of other experiments, which is probably caused by the migration of the fines toward the filter or by fines blocking the filter cloth. The fit of Eq. 12 is based on the specific cake-resistance values at the end of the experiment (22 to 24 hours). Because the specific cake resistance increases during the experiment, the values used for the fit of Eq. 12 are too high. Consequently, the model prediction of the mass fraction of solids in Figure 8 is lower than the experimental curve. The fit of Eq. 12 was optimized by adapting the parameter α_0 to the experiment, keeping the value of d constant. This led to the optimum value of $\alpha_0 = 0.35\times10^9$ m/kg, which is a reduction by a factor of 3.7 compared to the original fit. It appears from Figure 4 that at the end of the permeability measurement (22 to 24 hours) the specific cake resistance is on average a factor of 2.5 higher than at the time where the in- and outlet flows are equal. Since it takes 5 hours on average before the flows equalize, it is not unrealistic that the specific cake resistance is a factor of 3.7 lower than the value at the end of the experiment, after an expression time of 1 hour.

Simulations at other conditions were carried out with the optimal values of α_0 and d. The effect of the expression time and the solids load on the porosity distribution is shown in Figures 9 and 10. From Figure 9 it appears that the influence of the expression time can be described reasonably well, even at an expression time of 17 hours. From Figure 10 it follows that there is no systematic increase of the difference between model and experiment at different solids loads, which indicates that the trend of the experimental curves can be described well. Simulations of the expression step are shown in Figure 11 at various externally applied pressures. It appears that the modeled porosity distributions are not influenced further by the pressure at pressures higher than 4.7 bar. Because previous research has shown that the accuracy of the simulations is assured, this phenomenon is not a numerical artefact. Since the mass fraction of solids at the filter

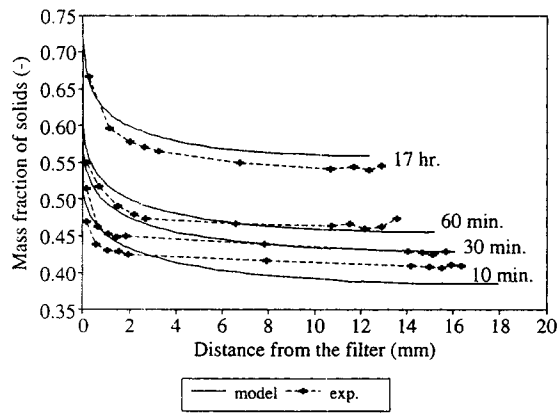

Figure 9. Simulations using the permeability equation (Eq. 12), with $\alpha_0 = 0.35\times10^9$ m/kg vs. experiments as a function of the expression time.

Solids load = 7.07×10^{-3} $m^3_{solids}/m^2_{filter}$; pressure = 10.7 bar.

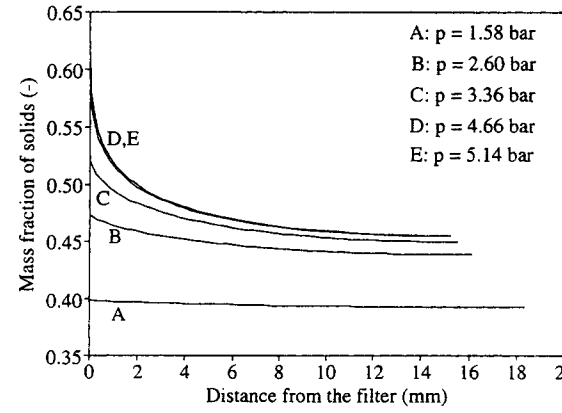

Figure 11. Porosity gradients as a function of the externally applied pressure.

Simulation conditions: permeability equation (Eq. 12), with $\alpha_0 = 0.35\times10^9$ m/kg, expression time = 3,600 s; solids load = 7.07×10^{-3} $m^3_{solids}/m^2_{filter}$.

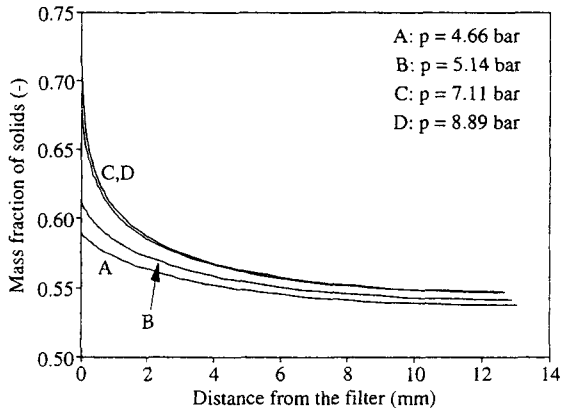

Figure 12. Influence of a lower value of $\alpha_0 = 0.35 \times 10^8$ m/kg, using permeability equation (Eq. 12) on the modeled porosity distribution as a function of the externally applied pressure.

Expression time = 3,600 s; solids load = 7.07×10^{-3} $m^3_{solids}/m^2_{filter}$.

increases with pressure, the specific cake resistance also increases. This increasing resistance leads to a proportional increase in the gradient of the solid compressive pressure because the velocities at the filter are equal. The specific cake resistance at the filter follows from extrapolation of Eq. 12. The pressure at which the mass fraction of solids is not affected further is therefore dependent on the fit of the permeability equation. The existence of this limiting pressure has been confirmed experimentally, but at much higher pressures than 4.7 bar. The modeling results also indicate that a limiting pressure may exist for other materials with high compressibility and a permeability strongly dependent on porosity.

Figure 12 shows the effect of a lower cake resistance (decrease of α_0 by a factor 10). On comparison with Figure 11, it appears that the pressure, at which the mass fraction of solids is not affected further, increases. Consequently, a decrease in the cake resistance has two effects: (1) a higher mass fraction of solids at the same pressure, and (2) a higher pressure at which the mass fraction of solids is not additionally affected. A decrease in the specific cake resistance can be obtained by removing the fines from the slurry.

Conclusions

In this work, experimental and modeling results of the permeability of a highly compressible viscoelastic material are presented. These results are combined with compressibility data, leading to a model for the expression step.

The permeability of palm-oil filter cakes was measured with both air and filtered palm oil. These measurements suggested that permeability increases by a factor of 200 if all the particles smaller than 150 μm are removed.

During the liquid permeability measurements the specific cake resistance increases more than would be expected from consolidation of the cake alone. This increase is probably caused by the migration of the fines toward the filter or by fines blocking the filter. Removing small particles from the slurry before expression leads to a significant increase in the solid-phase content during expression, which is caused by the higher permeability.

From the results of modeling the expression step it appeared that a pressure exists for palm-oil filter cakes, above which the modeled mass fraction of solids is not influenced further. This limiting pressure is dependent on the specific cake resistance at the filter. A decrease in the specific cake resistance has two effects: (1) a higher mass fraction of solids at the same pressure, and (2) a higher pressure at which the mass fraction of solids is not affected further. A limiting pressure is possibly caused by the combination of the high compressibility with a specific cake resistance that is strongly dependent on porosity.

Acknowledgment

The authors are grateful to the Unilever Research Laboratory, Vlaardingen, for their financial support.

Literature Cited

Barends, F. B. J., *Consolidatie in grond*, Syllabus Symp. *Persfiltratie, de Theorie en de Praktijk*, Nederlandse Procestechnologen NPT (1994).

Barends, F. B. J., "Nonlinearity in Groundwater Flow," PhD Thesis, Delft Univ. of Technology, Delft, The Netherlands, p. 34 (1980).

Bronwell, A., *Advanced Mathematics in Physics and Engineering*, McGraw-Hill, New York, p. 102 (1953).

Chase, G. G., and M. S. Willis, "Compressive Cake Filtration," *Chem. Eng. Sci.*, **47**, 1373 (1992).

De Wiest, R. J. M., ed., *Flow Through Porous Media*, Academic Press, New York, p. 91 (1969).

Grace, H. P., "Resistance and Compressibility of Filter Cakes," *Chem. Eng. Prog.*, **49**, 303 (1953).

Happel, J., "Viscous Flow in Multiparticle Systems: Slow Motion of Fluids Relative to Beds of Spherical Particles," *AIChE J.*, **4**, 197 (1958).

Kamst, G. F., O. S. L. Bruinsma, and J. de Graauw, "Solid Phase Creep During the Expression of Palm Oil Filter Cakes," *AIChE J.*, **43**(3), 665 (1997).

Kamst, G. F., "Filtration and Expression of Palm Oil Slurries as a Part of the Dry Fractionation Process," PhD Thesis, Delft Univ. of Technology, Delft, The Netherlands, p. 18 (1995).

Moore, W. J., *Physical Chemistry*, Prentice-Hall, Englewood Cliffs, NJ, p. 17 (1972).

Shirato, M., T. Murase, M. Iwata, and S. Nakatsuka, "The Terzaghi-Voigt Combined Model for Constant-Pressure Consolidation of Filter Cakes and Homogeneous Semi-Solid Materials," *Chem. Eng. Sci.*, **41**(12), 3213 (1986).

Smiles, D. E., and J. M. Kirby, "Aspects of One-Dimensional Filtration," *Sep. Sci. Technol.*, **22**(5), 1405 (1987).

Stamatakis, K., and C. Tien, "Cake Formation and Growth in Cake Filtration," *Chem. Eng. Sci.*, **46**, 1917 (1991).

Tien, C., "Retention of Fine Particles within Filter Cakes in Cake Filtration," *J. Chin. Inst. Chem. Eng.*, **22**, 385 (1991).

Tiller, F. M., and C. S. Yeh, "The Role of Porosity in Filtration; Part XI: Filtration Followed by Expression," *AICHE J.*, **33**, 1241 (1987).

Willis, M. S., R. M. Collins, and W. G. Bridges, "Complete Analysis of Non-Parabolic Filtration Behaviour," *Chem. Eng. Res. Des.*, **61**, 96 (1983).

Manuscript received Feb. 21, 1996, and revision received Oct. 22, 1996.